

# Ex vivo 1H MR spectroscopy and histology after experimental chronic spinal cord compression

Stephan Duetzmann<sup>1</sup>, Ulrich Pilatus<sup>2</sup>, Volker Seifert<sup>1</sup>, Gerhard Marquardt<sup>1</sup>, Matthias Setzer<sup>1</sup>

<sup>1</sup>Department of Neurosurgery, <sup>2</sup>Brain Imaging Center, Central Research Facility, Goethe University, Frankfurt/Main, Germany

Correspondence to: Dr. Stephan Duetzmann, MD. Zentrum der Neurologie und Neurochirurgie, Schleusenweg 2-16, 60528 Frankfurt, Germany.

Email: stephan.duetzmann@gmail.com.

**Background:** Proton magnetic resonance imaging (MRS) is used increasingly to image the spinal cord in compressive cervical myelopathy (CSM). However, detailed analyses of the underlying histomorphological changes leading to MRS alterations are still lacking. The aim of our study was to correlate neuroimaging and neuropathologic alterations in a rabbit myelopathy model.

**Methods:** Chronic spinal cord compression was induced in a rabbit model (n=16) allowing for a gradual 270° compression of the spinal cord. Spinal cord compression core areas were divided into two samples for (A) 1H MRS and (B) histopathological analyses. Postoperatively the animals underwent a neurological examination twice a day and outcome was categorized in pattern of injury and amount of recovery.

**Results:** Three groups were observed and categorized: (I) animals with severe deficits and no or minimal recovery; (II) animals with severe deficits and complete or almost complete recovery; (III) animals with mild to moderate deficits and a complete recovery. Significant differences in the lesioned spinal cords between the different recovery groups were found for N-acetyl-aspartate and choline. NAA/Cr was detected significantly (P<0.001, ANOVA) less in the group that did show permanent neurological deficits. To the contrary, choline was detected significantly (P<0.001, ANOVA) more in the group that did show permanent neurological deficits. Histologically the first group showed more apoptosis and necrosis than the second and third group.

**Conclusions:** MR spectroscopy (MRS) may be helpful for clinicians in improving the prognostic accuracy in cervical myelopathies since this method nicely reflects the extent and severity of spinal cord damage.

**Keywords:** Subacute and chronic spinal cord compression; *ex vivo* 1H MR spectroscopy (MRS)

Submitted Nov 14, 2016. Accepted for publication Apr 22, 2017.

doi: 10.21037/jss.2017.05.08

View this article at: <http://dx.doi.org/10.21037/jss.2017.05.08>

## Introduction

Cervical spondylotic myelopathy (CSM) is a common cause of acquired spinal cord dysfunction in elderly and the most common cause of non-traumatic spastic para- and quadriplegia (1).

The response to decompression surgery can significantly vary among individuals (2). Thus, imaging methods for the non-invasive quantification of histopathological alterations associated with permanent neurological deficits are essential for the treating physician. Recently, considerable progress has been made in the neuroradiological diagnostics of

cervical spondylotic myelopathy by using MR spectroscopy (MRS) (3-9). MRS may predict the prognosis in patients with CSM. It has been shown that choline/N-acetyl aspartate ratio in the center of spinal cord lesions were correlated with patient outcome measured by mJOA (4).

Only few histological studies on patients with CSM exist. These show that the central gray and medial portions of the myelinated long tracts are affected most severely and show evidence of cystic cavitation, gliosis, and demyelination (10).

However, the underlying histopathological changes leading to MRS alterations are still unclear to date. To elucidate the effect of histomorphological changes in

myelopathy on MRS signals, we used a rabbit model of chronic spinal cord compression.

## Methods

### Experimental animals

Sixteen female New Zealand White rabbits were studied. The mean preoperative weight was  $3.1 \pm 0.2$  kg. All animals were kept in groups preoperatively and single postoperatively with free access to food and water.

### Procedures

Anesthesia was induced with ketamine and xylazine. After induction the animals were intubated and ventilated for the surgical procedure. Total intravenous anesthesia was maintained by 2% propofol. During anesthesia systemic arterial blood pressure, O<sub>2</sub> saturation and ECG was monitored continuously. Blood gas analyses were recorded regularly.

### Surgery

For this study a model recently developed by our group for subacute and chronic spinal cord compression was used. The surgical steps are described in detail elsewhere (11). Briefly, after induction of anesthesia animals were positioned prone for exposure of the upper thoracic spine. After midline skin incision paravertebral muscles were moved laterally and the vertebral lamina was exposed. Under the operating microscope on each side a small hole was drilled caudal to the articular process and a silicone ribbon was inserted through one hole, crossed over the midline and inserted in the other hole down top resulting in the formation of a loop. Thereafter the spinal dura mater was exposed by removing the lamina with a drill. By pulling at the ends of the ribbon the loop was brought into contact with the dura without exerting compression on the spinal cord. The ends of the silicone ribbon were inserted through two rubber tubes and the ends were secured with a hemoclip. Postoperatively the neurological status was checked twice a day.

Then, after 1 week, the skin incision was reopened and the loop and its ends with the hemoclips were reexposed. The loop was gradually tightened by pulling gently at one end of the ribbon and a new hemoclip was placed beneath the first clip, fixing the loop in its new position.

This resulted in a compressive effect on the spinal cord. If the animal did not exhibit a neurological deficit after an observation period of 1 week the tightening procedure was repeated. Once neurological deficits had evolved the spinal cord was decompressed by cutting one end of the band and removing the entire device. The compression and decompression procedures were carried out in sedation with ketamine and xylazine under spontaneous breathing of 100% O<sub>2</sub>. Pre- and postoperatively MR imaging was performed to document the compression and decompression of the spinal cord.

### Neurological examination

Postoperatively the animals underwent a neurological examination twice a day. The neurological grading was carried out according to Marquardt *et al.* (11): grade V, no motor deficits (rabbits able to run); grade IV, mild weakness (rabbits able to walk but not to run); grade III, moderate weakness (rabbits able to stand but not to walk); grade II, marked weakness (movements of the limbs visible but rabbits not able to stand); grade I, severe weakness (only slight movements of the limbs visible); and Grade 0, paraplegia.

### Tissue preparation

For the spectroscopic examinations pathological core areas of 16 animals were used. For this procedure the animals were intubated and deeply anesthetized with propofol and fentanyl. Muscle relaxation was achieved with pancuronium. The skin incision of the upper thoracic spine was opened again and the former interlaminar approach and the compression site (epicenter of injury) reexposed. The epicenter was removed en bloc. The bloc was cut in several (4,5) small segments. One half of the segments was quickly frozen in liquid nitrogen and stored at  $-80$  °C. The other segments were fixed in 4% paraformaldehyde, cryoprotected in 30% sucrose and frozen at  $-80$  °C or embedded in paraffin according to standard protocols.

### Ex vivo 1H MRS

The quickly frozen spinal cord segments (range, 30–170 mg wet weight) were homogenized adding 0.2–0.5 mL of chilled 6% perchloric acid (PCA) and centrifuged for 5 min at 16,000 g. The supernatant was collected and redissolved in PCA and centrifuged again for 5 min at 16,000 g. The

combined supernatant was carefully neutralized with KOH, centrifuged to remove precipitated  $\text{KClO}_4$ , lyophilized, and stored at  $-80^\circ\text{C}$ . The residual pellets were resuspended in 1 mL water, homogenized and neutralized with KOH. The suspension was lyophilized and stored at  $-80^\circ\text{C}$ . For the *in vitro* MRS examination, PCA extracts were redissolved in 0.5 mL deuterium oxide. The sample was then transferred into a 5 mm diameter sample tube. All spectra were recorded on a high-resolution NMR spectrometer (Bruker DRX 500, Bruker, Karlsruhe, Germany) operating at 11.75 Tesla. Proton spectra were collected at  $25^\circ\text{C}$  using a pulse acquired sequence. The spectral parameters were: 10,000 Hz spectral width, 16K data points,  $90^\circ$  pulse angle. Averaging 360 scans with a repetition time of 5 s resulted in a time of 30 min per spectral data set. The metabolite signal intensities of the injured spinal cord and motor cortex tissue were quantified (normalized) by calculating their ratio to the signal intensity of the Creatine signal (Cr). Values are given as mean  $\pm$  SD.

### Immunohistochemistry

After removal the blocs were fixed by immersion in 4% paraformaldehyde (pH 7.4, for around 2 days on a rotator), and afterwards cryoprotected in Tris buffered saline (TBS, pH 7.4) containing 30% sucrose. Then the blocks were frozen and cut into 100  $\mu\text{m}$  thick horizontal (spinal cord) sections on a cryostat. Free-floating sections were rinsed in TBS after each step of the incubation procedure (10 minutes). Non-specific staining was reduced by two preincubation steps: (I) 10% methanol and 7% hydrogen peroxide in TBS; (II) 1.5% lysine, 0.25% triton X-100 and 10% bovine serum albumin (BSA) (all from Sigma, St. Louis, MO, USA) in TBS (60 minutes). Then the sections were incubated in the primary antibody at  $4^\circ\text{C}$  for 2 days (mouse anti-Myelin Basic Protein (MBP), Sternberger Monoclonals Inc., Baltimore, MD, USA diluted 1:1,000). Afterwards, the sections were incubated with the biotinylated secondary antibody (secondary anti-mouse IgG, Vector Laboratories Burlingame, USA); diluted 1:200 in TBS with 2% BSA for 2 h at room temperature and thereafter transferred to the avidin-biotin-peroxidase complex (ABC, Vector laboratories diluted 1:25 in TBS) for another 2 hours. To visualize the immunoreaction product, the chromogene 3,3'-diaminobenzidine-tetra hydrochlorid (DAB, Sigma, 0.07% in TBS with 0.003% hydrogen peroxide) was used. Finally the sections were mounted on gelatin-coated slides dehydrated in a graded

series of alcohol, cleared in xylene, mounted on slides and coverslipped with DePeX (Serva, Heidelberg, Germany).

### Histology

Histological Sections were analysed on after HE staining for general appearance of apoptosis, necrosis, edema, microglial proliferation, astrogliosis, astrospheroids, bleeding and neuronal cell loss. An experienced blinded neuropathologist graded severity of each of these characteristics into 4 arbitrary grades (grade 4 representing the most severe).

## Results

### Clinical characteristics

At the end of the study we observed that the animals could be classified into three groups: (I) animals that initially had a severe neurologic deficit (Grade III and higher) and did not recover; (II) animals that initially had a severe neurologic deficit and did recover to Grade IV or lower; (III) animals that initially had a light deficit.

Of the 16 animals, 3 animals were clinically classified into grade III (severe deficit, bad recovery), 7 animals were classified into grade II (severe deficit, good recovery), 6 animals were classified into grade I (mild deficit).

### Neurological recovery groups and relative metabolite concentrations

Significant differences in the lesioned spinal cords between the different recovery groups were found for N-acetyl-aspartate and choline. NAA/Cr levels were significantly ( $P < 0.001$ , ANOVA) lower in the group that did show permanent neurological deficits. NAA was detected slightly increased in animals that recovered from a severe deficit and even higher in animals that did not have a severe deficit (*Figure 1A*). To the contrary, choline was detected significantly ( $P < 0.001$ , ANOVA) more in the group that did show permanent neurological deficits. Slightly decreased choline was detected in animals that recovered from a severe deficit and even less in animals that did not have a severe deficit (*Figure 1B*).

Histologically the first group showed more apoptosis and neuronal cell loss than the second and third group (*Figure 2, Table 1*). Apoptosis was observed significantly more severe in the group that did not recover than in the groups that did recover. Neuronal cell loss was less discriminatory

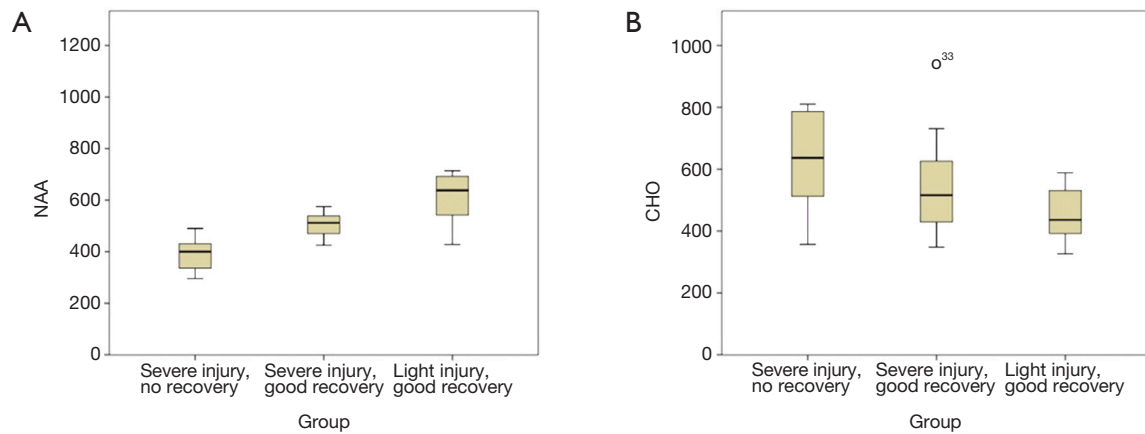


**Figure 1** NAA and choline were measured in animals. (A) Boxplot of mean spectroscopically measured NAA as a marker of neuronal cell integrity stratified between the 3 groups; (B) boxplot of mean spectroscopically measured choline as a surrogate marker of myelin content stratified between the 3 groups.

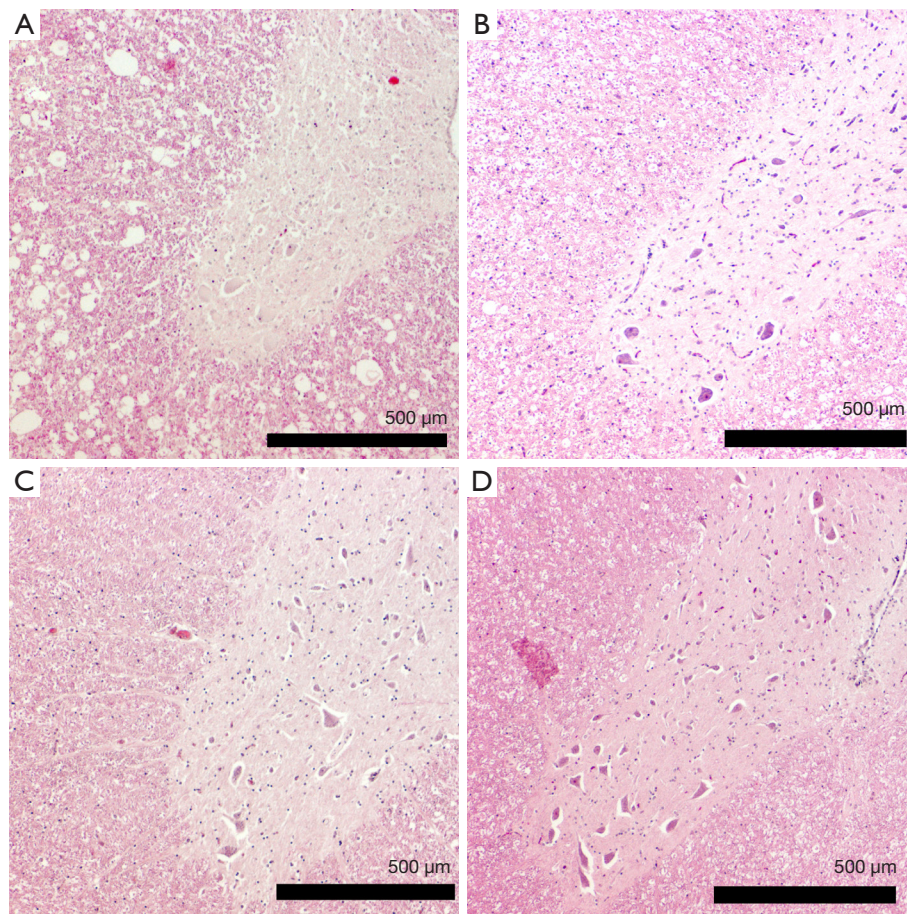


**Figure 2** Four representative HE images. (A) Group 1 showing neuronal cell loss; (B) group 2; (C) group 3; (D) normal rabbit.

being most severe in the group that did not recover than in the other two groups. Necrosis was not observed, except in one animal of group 1. Furthermore, in the group with permanent deficits the Myelin staining showed typically round lesions that appeared as punched out. The group that

showed severe deficits and recovered and the group that showed only mild deficits did not display these lesions, but had a moderate reduction in myelin staining (Figures 3,4). Edema, microglial proliferation, astrogliosis and astrospheroids were observed but did not differ between the groups. Bleeding was not observed.

**Table 1** Mean graded pathological characteristics of HE stained spinal cord core damage areas

Group	Apoptosis	Neuronal cell loss
1	3.3±0.8	2.3±0.5
2	2.2±0.4	1.4±0.5
3	2.4±0.4	2.0±0.4

Group 1: animals that initially had a severe neurologic deficit (grade III and higher) and did not recover; group 2: animals that initially had a severe neurologic deficit and did recover to Grade IV or lower; group 3: animals that initially had a light deficit. An experienced blinded neuropathologist graded severity of each of these characteristics into 4 arbitrary grades (grade IV representing the most severe).

## Discussion

One of the major challenges in spine surgery of patients with advanced cervical spondylosis is distinguishing between patients who will benefit from a spine surgery or not. Furthermore even after surgery patient counseling regarding their prognosis is difficult, since some patients recover earlier than others (12). Biochemical markers such as serum S100b and NSE have a prognostic relevance in the event of acute or subacute spinal cord compression (13,14) but not if the spinal cord is compressed chronically (15). Accordingly serial S100b and NSE serum measurements in surgically treated patients with cervical myelopathy do not have any prognostic significance (16). Standard MRI can appear quite similar between asymptomatic and

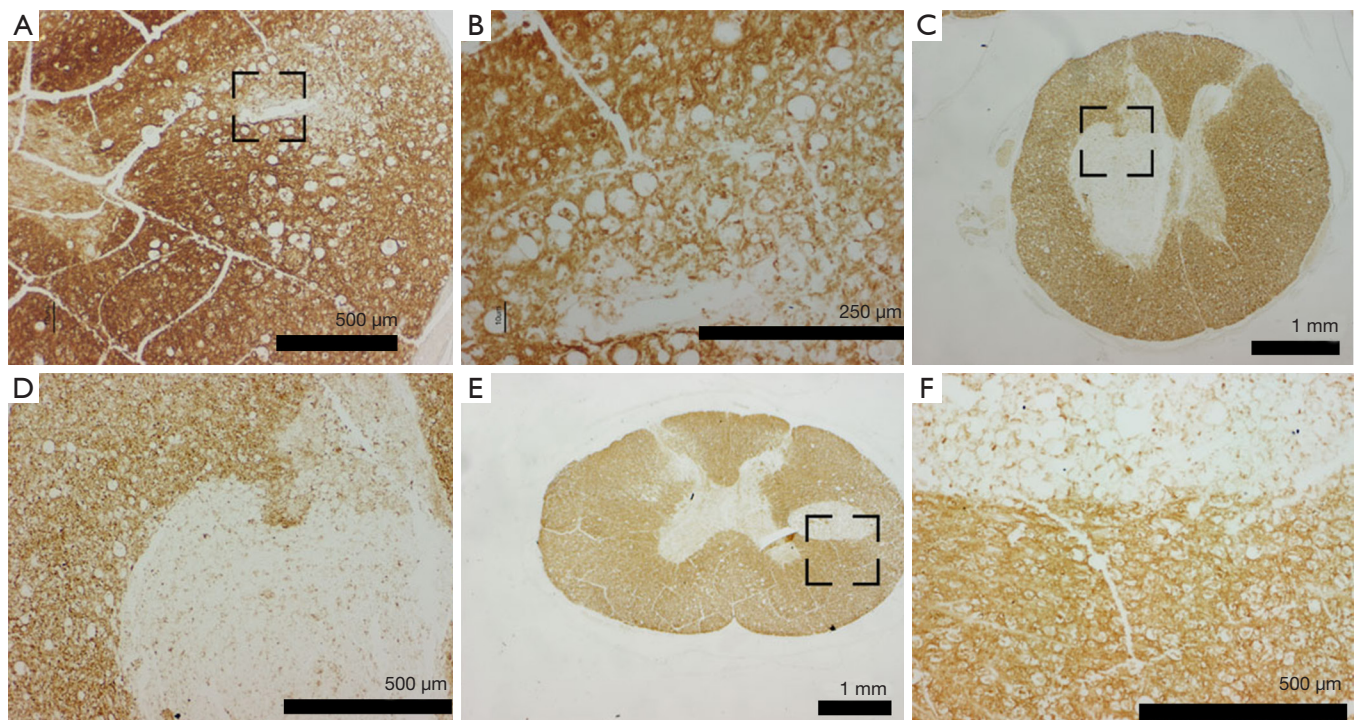


**Figure 3** Representative images of the myelin basic protein staining. (A,B) The typical pattern of myelin basic protein loss but no punched out lesion in animals that made a good recovery (group 2 and 3); (C-F) the typical pattern of punched out lesions in animals that did not recover well.

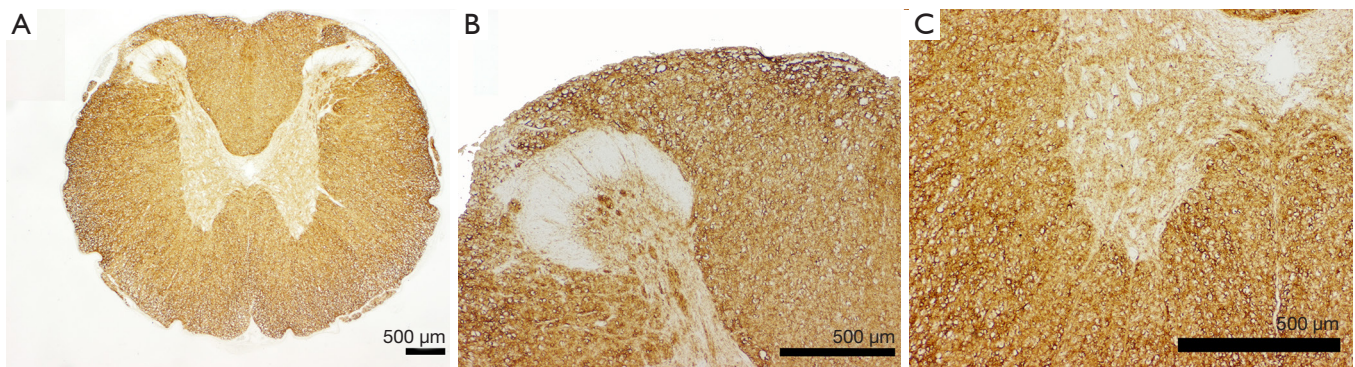


**Figure 4** For comparison displayed is a normal finding.

symptomatic individuals (17). Bilateral T2 hyperintensity within the central cord has previously been shown to correlate with current mJOA and suspected neurological damage (6). It also has been associated with worse prognosis after decompression surgery (18). Still more reliable and accurate markers are lacking.

Recent studies have suggested that MRS techniques may be valuable for assaying microstructural and biochemical information related to degeneration and metabolic dysfunction, and provide more sensitive identification of spinal cord injury than standard MRI (3,4,9). Still these human studies cannot correlate their results with reliable pathomorphological data displaying what is really going on in the spinal cord.

Therefore, our previously established model of chronic spinal cord compression in rabbits may help to further elucidate this.

We hypothesize that the reduction in the NAA signal reflects the demise of alpha motoneurons after chronic spinal cord compression, since NAA is a marker that typically reflects the viability of neurons (19). This hypothesis is supported by the death of cells seen histologically. This finding also explains that the animals did not recover, because the cells were ultimately lost.

The decrease in choline in the animals that did not recover can be explained by loss of myelin. As demonstrated in the myelin staining, some myelin is lost in the groups that did recover from the compression and punched out myelin lesions appeared in the groups that did not recover. Choline is an important part of the cell membrane and therefore should be reduced if myelin is lost (20). Therefore the reduction of choline seems to reflect the loss of myelin in our model.

Previously it has been shown that MRS can play an

important role in the management and prognosis of patients with CSM (4,6,7,9,21-23). Our studies show that morphological changes are correlated with a change in the concentration of metabolites, which can also be detected with *in vivo* MRS. Thus MRS should provide a tool to evaluate the morphological damage. Unfortunately the group around Holly *et al.* encountered technical difficulties in measuring at the site of compression (4). Instead they preoperatively measured more proximally at C2 and saw indirect signs of Wallerian Degeneration (which they could correlate well with mJOA outcome).

Our studies suggest that a post-operative MRS measurement at the site of compression may reflect axonal integrity and neuronal viability and help in determining the prognosis of these patients. Therefore further clinical post-operative studies are necessary.

The limitations of our studies are that we measured neuronal cell demise only subjectively. The assessment, however, was blinded and performed by an expert. However in a previous study using cell counting and Nissl staining, we could show clearly a measurable demise of cells (24). Furthermore we did not quantitatively measure myelin content. Lastly the animal model of chronic spinal cord compression may represent a rather subacute compression than a chronic one and confers all the limitations that come along with every animal model of human disease (biomechanics, etc.). This has been discussed extensively previously in the context of the first description of the model (11,25).

### Acknowledgements

We deeply thank Prof. Michel Mittelbronn and Conny Zachskorn for slide analysis, tissue preparation and HE

staining of the rabbits.

The study was funded by the University of Frankfurt.

### Footnote

*Conflicts of Interest:* The authors have no conflicts of interest to declare.

*Ethical Statement:* Approval was given by the local animal care committee of the Regierungspräsident Darmstadt (Ge Nr.138 F).

### References

- Baptiste DC, Fehlings MG. Pathophysiology of cervical myelopathy. *Spine J* 2006;6:190S-197S.
- Dokai T, Nagashima H, Nanjo Y, et al. Surgical outcomes and prognostic factors of cervical spondylotic myelopathy in diabetic patients. *Arch Orthop Trauma Surg* 2012;132:577-82.
- Ellingson BM, Salamon N, Grinstead JW, et al. Diffusion tensor imaging predicts functional impairment in mild-to-moderate cervical spondylotic myelopathy. *Spine J* 2014;14:2589-97.
- Ellingson BM, Salamon N, Hardy AJ, et al. Prediction of Neurological Impairment in Cervical Spondylotic Myelopathy using a Combination of Diffusion MRI and Proton MR Spectroscopy. *PLoS One* 2015;10:e0139451.
- Ellingson BM, Salamon N, Holly LT. Advances in MR imaging for cervical spondylotic myelopathy. *Eur Spine J* 2015;24 Suppl 2:197-208.
- Ellingson BM, Salamon N, Woodworth DC, et al. Correlation between degree of subvoxel spinal cord compression measured with super-resolution tract density imaging and neurological impairment in cervical spondylotic myelopathy. *J Neurosurg Spine* 2015;22:631-8.
- Holly LT, Ellingson BM, Salamon N. Metabolic Imaging Using Proton Magnetic Spectroscopy as a Predictor of Outcome Following Surgery for Cervical Spondylotic Myelopathy. *Clin Spine Surg* 2016. [Epub ahead of print].
- Holly LT. Management of cervical spondylotic myelopathy with insights from metabolic imaging of the spinal cord and brain. *Curr Opin Neurol* 2009;22:575-81.
- Holly LT, Freitas B, McArthur DL, et al. Proton magnetic resonance spectroscopy to evaluate spinal cord axonal injury in cervical spondylotic myelopathy. *J Neurosurg Spine* 2009;10:194-200.
- Ogino H, Tada K, Okada K, et al. Canal diameter, anteroposterior compression ratio, and spondylotic myelopathy of the cervical spine. *Spine (Phila Pa 1976)* 1983;8:1-15.
- Marquardt G, Setzer M, Theisen A, et al. A novel dynamic model for experimental spinal cord compression. *J Neurosurg Spine* 2005;2:466-71.
- Matz PG, Holly LT, Mummaneni PV, et al. Anterior cervical surgery for the treatment of cervical degenerative myelopathy. *J Neurosurg Spine* 2009;11:170-3.
- Marquardt G, Setzer M, Seifert V. Protein S-100b for individual prediction of functional outcome in spinal epidural empyema. *Spine (Phila Pa 1976)* 2004;29:59-62.
- Marquardt G, Setzer M, Seifert V. Serum biomarkers for experimental acute spinal cord injury: rapid elevation of neuron-specific enolase and S-100 beta. *Neurosurgery* 2006;58:E590; author reply E590.
- Marquardt G, Setzer M, Szelenyi A, et al. Prognostic relevance of serial S100b and NSE serum measurements in patients with spinal intradural lesions. *Neurol Res* 2009;31:265-9.
- Marquardt G, Setzer M, Szelenyi A, et al. Significance of serial S100b and NSE serum measurements in surgically treated patients with spondylotic cervical myelopathy. *Acta Neurochir (Wien)* 2009;151:1439-43.
- Suk KS, Kim KT, Lee JH, et al. Reevaluation of the Pavlov ratio in patients with cervical myelopathy. *Clin Orthop Surg* 2009;1:6-10.
- Mizuno J, Nakagawa H, Inoue T, et al. Clinicopathological study of "snake-eye appearance" in compressive myelopathy of the cervical spinal cord. *J Neurosurg* 2003;99:162-8.
- Moffett JR, Ross B, Arun P, et al. N-Acetylaspartate in the CNS: from neurodiagnostics to neurobiology. *Prog Neurobiol* 2007;81:89-131.
- Weidensteiner C, Allegrini PR, Sticker-Jantschke M, et al. Tumour T1 changes in vivo are highly predictive of response to chemotherapy and reflect the number of viable tumour cells--a preclinical MR study in mice. *BMC Cancer* 2014;14:88.
- Holly LT, Dong Y, Albistegui-DuBois R, et al. Cortical reorganization in patients with cervical spondylotic myelopathy. *J Neurosurg Spine* 2007;6:544-51.
- Holly LT, Moftakhar P, Khoo LT, et al. Surgical outcomes of elderly patients with cervical spondylotic myelopathy. *Surg Neurol* 2008;69:233-40.
- Holly LT, Matz PG, Anderson PA, et al. Clinical prognostic indicators of surgical outcome in

- cervical spondylotic myelopathy. *J Neurosurg Spine* 2009;11:112-8.
24. Marquardt G, Setzer M, Theisen A, et al. Experimental subacute spinal cord compression: correlation of serial S100B and NSE serum measurements, histopathological changes, and outcome. *Neurol Res* 2011;33:421-6.
25. Marquardt G, Setzer M, Seifert V. Protein S-100b as serum marker for prediction of functional outcome in metastatic spinal cord compression. *Acta Neurochir (Wien)*

2004;146:449-52.

---

*Contributions:* (I) Conception and design: M Setzer, G Marquardt, S Duetzmann; (II) Administrative support: V Seifert; (III) Provision of study materials or patients: M Setzer, S Duetzmann; (IV) Collection and assembly of data: M Setzer, S Duetzmann, U Pilatus; (V) Data analysis and interpretation: M Setzer, S Duetzmann, U Pilatus; (VI) Manuscript writing: All authors; (VII) Final approval of manuscript: All authors.

**Cite this article as:** Duetzmann S, Pilatus U, Seifert V, Marquardt G, Setzer M. *Ex vivo* 1H MR spectroscopy and histology after experimental chronic spinal cord compression. *J Spine Surg* 2017;3(2):176-183. doi: 10.21037/jss.2017.05.08